Article

Adsorption and Hysteresis of Bisphenol A and 17#-Ethinyl Estradiol on Carbon Nanomaterials

Bo Pan, Daohui Lin, Hamid Mashayekhi, and Baoshan Xing

Environ. Sci. Technol., **2008**, 42 (15), 5480-5485 • DOI: 10.1021/es8001184 • Publication Date (Web): 28 June 2008

Environ. Sci. Technol. **2008,** *42,* 5480–5485

Adsorption and Hysteresis of Bisphenol A and 17α-Ethinyl Estradiol on Carbon Nanomaterials

BO PAN, DAOHUI LIN, HAMID MASHAYEKHI, AND BAOSHAN XING*

Department of Plant, Soil and Insect Sciences, University of Massachusetts, Amherst, Massachusetts 01003

Received January 13, 2008. Revised manuscript received May 7, 2008. Accepted May 12, 2008.

Adsorption of 17α-ethinyl estradiol (EE2) and bisphenol A (BPA) on carbon nanomaterials (CNMs) was investigated. Single point adsorption coefficients (*K*) showed significant relationship with specific surface areas of CNMs for both chemicals, indicating surface area is a major factor for EDC adsorption on CNMs. BPA adsorption capacity is higher than EE2 on fullerene and single-walled carbon nanotubes (SWCNT). Our molecular conformation simulation indicated that BPA has a unique ability to adsorb on the curvature surface of CNMs because of its "butterfly" structure of two benzene rings. The higher adsorption capacity of BPA over EE2 is well explained by considering helical (diagonal) coverage of BPA on the CNMs surface and wedging of BPA into the groove and interstitial region of CNM bundles or aggregates. The comparison of K_{HW} (hexadecane-water partition coefficient) normalized adsorption coefficients between EDCs and several polyaromatic hydrocarbons indicates that $\pi-\pi$ electron donor−acceptor system is an important mechanism for the adsorption of benzene-containing chemicals on CNMs. The high adsorption capacity and strong desorption hysteresis of both chemicals on SWCNT indicate that SWCNT is a potential adsorbent for water treatment.

Introduction

Endocrine disrupting chemicals (EDCs) can mimic the biological activity of natural hormones, occupy (but not active) the hormone receptors, or interfere the transport and metabolic processes of natural hormones. Thus, this type of chemicals interferes the reproductive systems of wildlife and humans (*1*). A great number of EDCs are synthetic pharmaceuticals for humans and livestock. Absorption efficiency of these pharmaceuticals is generally low, and the original or conjugated chemicals were excreted and discharged into water (*2*). Therefore, the main source of EDCs is municipal sewage (*3*), and it is of essential importance to optimize the removal processes for water treatment.

Efficiency of EDC removal has been examined using active sludge (*4*), colloids derived from active sludge (*5*), minerals (*6*), active carbon of various origins (*7–11*), and hybrid particles (*12*). Because of different EDC properties, poor removal was observed for several compounds (*13*). EDCs were detected in the effluents of sewage treatment plants, indicating failure for these plants to remove EDCs (*14*). Thus, further research is needed to enhance the efficiency of EDC removal in water treatment using an adsorbent with higher removal performance, optimized disposal process, or the combination of both.

Among new materials which have potential as an adsorbent for water treatment, carbon nanomaterials (CNMs) have shown high adsorption capacity for polyaromatic hydrocarbons (*15*), pesticides (*16*), natural organic matter (*17*), heavy metals (*18*), and floride (*19*). Cai et al. indicated that multiwalled carbon nanotubes could extract EDCs from aqueous phase more efficiently than C_{18}, and thus could be used as a packing material in solid phase extraction for a simple, rapid, and reliable extraction method (*20*). However, adsorption characteristics of EDCs on CNMs have not been investigated extensively. Among EDCs, 17α-ethinyl estradiol (EE2) and bisphenol A (BPA) are the two compounds most frequently studied in environmental research. EE2 is widely used as an oral contraceptive, and its toxicity has a potency 10−50 folds higher than estrone (El) and 17β-estradiol (E2) (*21*), but, low EE2 removal was observed (*22*). BPA is used as a monomer for production of polycarbonate and epoxy resin (*23*), which are widely used in human daily life. However, significant disordering of wildlife endocrine system has been reported at environmental relevant BPA concentrations (*24*). The solubility of BPA in water is 50 times higher than EE2 (Table SI, Supporting Information), and thus these two chemicals could represent EDCs with properties of a wide range. Therefore, we used EE2 and BPA as two model EDCs, and studied their adsorption characteristics on CNMs. The goal of this work was to determine the adsorption capacity and mechanisms of EE2 and BPA by CNMs.

Experimental Section

Carbon Nanomaterials. CNMs used in this study were single-walled (SWCNT) and three multiwalled carbon nanotubes (MWCNTs) and fullerene. Fullerene (purity > 99.5%) was obtained from Aldrich Chemical Co., and SWCNT (purity > 90%) and MWCNTs (purity > 95%) were purchased from Chengdu Organic Chemistry Co., Chinese Academy of Sciences. MWCNTs were MWCNT15, MWCNT30, and MWCNT50 with outer diameters of 8−15, 20−30, and 30−50 nm, respectively. The detailed structural properties were published previously (*15*). Carbon nanotubes (CNTs) used in this study were synthesized in the CH_4/H_2 mixture at 700 °C by the chemical vapor deposition method. The synthesized CNTs were purified by mixed HNO_3 and H_2SO_4 solutions to reduce the contents of metal catalyst and amorphous carbon. Activated carbon from wood charcoal was purchased from Fisher Scientific.

Adsorption Experiment. EE2 (3.38 g L^{-1}) and BPA (100 g L^{-1}) were dissolved in methanol separately as stock solutions. The adsorption experimental sequence was as Pan et al. (*25*). Briefly, the stock solutions were diluted sequentially to a series of concentrations distributed evenly on a log scale using 0.01 M $CaCl_2$ and 200 mg/L NaN_3 solution. The initial concentrations for the adsorption experiments were 100−3000 μg/L for EE2 and 100−40 000 μg/L for BPA. The solid/water (w/v) ratios were 1:100−1:200 for fullerene, and 1:20 000−1:120 000 for CNTs and activated carbon. The volume ratio of methanol to water was below 0.001 to avoid cosolvent effect. The vials containing the EDC solution and CNM or activated carbon were sealed with Teflon-lined stoppers immediately. The same concentration sequence of EDC solution without CNMs was run in the identical condition as reference. Headspace was kept minimal to reduce solute vapor loss. The vials were kept in dark and rotated vertically on a rotator

* Corresponding author phone: 413-545-5212; fax: 413-545-3958; e-mail: bx@pssci.umass.edu.

10.1021/es8001184 CCC: $40.75
Published on Web 06/28/2008

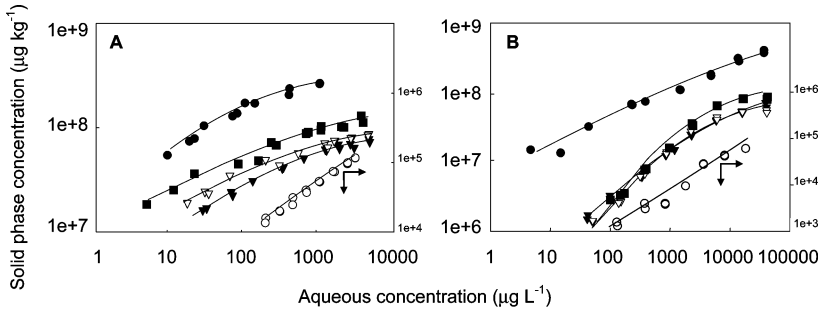

FIGURE 1. Adsorption isotherms of EE2 (A) and BPA (B) on CNMs. Solid lines are the fitting curves using PMM. The fitting results are listed in Supporting Information Table SII. Closed circles (●) are for SWCNT, and open circles (○) for fullerene. Closed squares (■), open triangles (△), and closed triangles (▲) are for MWCNT15, MWCNT30, and MWCNT50, respectively. Adsorption on fullerene is expressed on the right-side *y*-axis as indicated by the arrows.

(30 rpm, Glas-Col laboratory rotator) for 7 days, and centrifuged at 1000*g* for 15 min. According to our preliminary study, both adsorption and desorption reached equilibrium within 7 days. The supernatant was sampled for HPLC analysis. Sorbed chemicals were calculated by mass difference between original (C_0) and equilibrated concentrations (C_e). All experiments including the blanks were run in duplicate.

Detection of EE2 and BPA. Supernatant of each sample was transferred to a 2 mL HPLC vial and analyzed using HPLC. The mobile phase was 50:50 (v:v) of acetonenitrile and deionized water with 1% acetic acid. EE2 was analyzed with a fluorescence detector at 206 nm (excitation wavelength) and 310 nm (emission wavelength). The detection limit was 5 μg L^{-1}. BPA was quantified on a fluorescence detector at 220 nm (excitation wavelength) and 350 nm (emission wavelength) for the concentration range of 5−4000 μg L^{-1}, and on a UV detector at 280 nm for the samples with concentrations higher than 4000 μg L^{-1}.

Data Analysis. Different models were employed to fit the adsorption isotherms:

$$\text{Freundlich model (FM): } S_e = K_F \times (C_e)^n \quad (1)$$

$$\text{Polanyi−Mane mode(PMM): } S_e = S_P{}^0 \times \exp(Z \times (RT \ln(C_s/C_e))^d) \quad (2)$$

$$\text{Langmuir model (LM): } S_e = S_L{}^0 \times b \times C_e/(1 + b \times C_e) \quad (3)$$

where S_e is the solid-phase concentration of EE2 and BPA (μg kg^{-1}), and $S_P{}^0$ and $S_L{}^0$ are the adsorption capacities from PMM and LM, respectively. C_e represents the aqueous-phase concentration of solute (μg L^{-1}), whereas C_s stands for solubility at 20 °C (7600 μg L^{-1} for EE2 and 380 000 μg L^{-1} for BPA according to our measurements). K_F and n are the Freundlich adsorption parameters, Z and d are PMM adsorption constants and b (L μg^{-1}) is LM adsorption affinity constant. R is universal gas constant (8.314 × 10^{-3} kJ mol^{-1} K^{-1}), and T is absolute temperature (K).

Because the standard coefficient of determination (r^2) is affected by the number of fitting parameters and data points, adjusted coefficient of determination ($r_{adj}{}^2$) was calculated in order to compare the performance of the different models (*26*):

$$r_{adj}{}^2 = 1 - r^2(m^2 - b)/(m - 1)$$

where m is the number of data points used for fitting, and b the number of coefficients in the fitting equation.

Molecular Conformation Simulation. Molecular conformation changes were simulated using ChemBioOffice 2008. The 3-dimensional molecular structures were optimized using molecular mechanics theory (MM2) (*27*). Steric energies (including stretch, bend, stretch−bend, torsion, non-1,4 van der Waals, 1,4 van der Waals, and dipole/dipole energies) of other possible structures were also calculated in order to discuss the possibility of conformational changes.

Results and Discussion

Adsorption Sites of EDCs on CNMs. Freundlich model generally failed to describe the adsorption isotherms because of a bell-shaped error distribution (Figures S1−S3, Supporting Information), indicating that the adsorption data cannot be described properly by this model. The fitting results of the adsorption isotherms using Polanyi−Mane (PMM, Figure 1) and Langmuir models (LM, Supporting Information Figures S4−S5) are listed in Supporting Information Table SII. Better fitting was observed for PMM as identified by the higher $r_{adj}{}^2$ (0.975−0.994 for EE2 and 0.954−0.994 for BPA) and random error distribution. Therefore, the following discussion is based on the adsorption parameters calculated from PMM fitting.

Single point adsorption coefficient, K, was calculated at $C_e = 0.01\ C_s$ based on the fitting results using PMM, and is also listed in Supporting Informaton Table SII. A significantly positive correlation was observed between surface area and K ($C_e = 0.01 C_s$), for both EE2 and BPA ($r = 0.999$ at $P < 0.01$ for both chemicals, Supporting Information Figure S6), indicating surface area is a major factor for EDC adsorption on CNMs. The K values for EE2 were more than 1 order of magnitude higher than those for BPA on corresponding CNMs, consistent with their hydrophobicity difference (Supporting Information Table SI). However, BPA sorption capacities ($S_P{}^0$) were comparable or higher than EE2 with the biggest difference observed for fullerene (11 times higher for BPA over EE2). The difference generally decreased as CNM diameter increased (Figure 2). This phenomenon indicates that although the availability of surface sorption sites controls EE2 and BPA adsorption on CNMs, how these two types of molecules occupy the sorption sites is different. The types of adsorption sites on CNMs and molecular conformation of EDCs should be considered.

According to our previous study, inner pores of these CNTs are not available for adsorption because of the amorphous carbon and metals on both ends (*15*). Thus, three types of adsorption sites are available for adsorption on CNM bundles or aggregates, including surface, groove area, and interstitial pores (Figure 3). Zhao et al. reported that adsorption energy and charge transfer of several small molecules in groove and interstitial sites of the bundles are much higher than those on the surface area, because of the increased number of CNMs interacting points with sorbate molecules (*28*). In our study, CNMs were not sonicated and most of them would be present as bundles or aggregates. Therefore, groove and interstitial areas are of the major importance for EE2 and BPA adsorption.

The 3-dimensional structures for both chemicals were optimized based on steric energy and are presented in Supporting Information Figure S7. The two benzene rings in

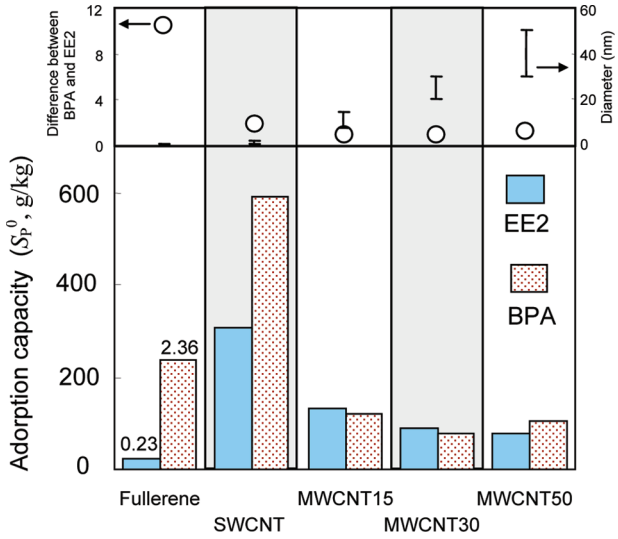

FIGURE 2. Comparison of adsorption capacity (S_P^0) for EE2 and BPA. The lower panel shows the direct comparison between EE2 and BPA for different CNMs. The upper panel shows the times of differences in S_P^0 (○) and in the outer diameters of CNMs (bars). The largest difference between EE2 and BPA adsorption were observed for fullerene and SWCNT, which have the smallest diameters.

BPA molecule attach to a carbon atom through a single bond, thus they could be easily rotated and form various angles. BPA molecule could wedge into the groove region because of its "butterfly" structure (BPA 3 and 5 in Figure 3), but EE2 molecule does not have this benefit. Contribution of groove region to the overall sorption sites would be lower for the CNMs with higher diameter, thus adsorption difference between EE2 and BPA for CNMs with higher diameters was lower as shown in Figure 2. In addition, a high contribution of groove area is expected for fullerene because of its small diameter and spherical surface (Figure 3). Therefore, the biggest difference between adsorption capacities of EE2 and BPA is observed for fullerene.

The interstitial area is in the middle of bundles or aggregates. In the comparison of molecular size, the size of the interstitial areas of fullerene and SWCNT is too small for both of the chemicals to fit into (Figure 3). Similarly, Pearce et al. did not observed any occupation of He atoms in interstitial area of SWCNT (*29*). As the diameter of CNMs increases, the interstitial area would be enlarged and available for adsorption. The shape of this area is similar to the groove area, and BPA molecules could wedge into these adsorption sites. Therefore, the difference between EE2 and BPA on MWCNT50, the one with the biggest diameter, increased (Figure 2).

The third adsorption site is on the surface of CNTs. The two benzene rings in BPA molecule could be adsorbed on CNT surface area parallel with the tube axis, around the circumference, or in diagonal direction (Figure 3). If both benzene rings of BPA attach on CNTs in the direction of tube axis, they have to stay in a same flat plane (BPA 1 in Figure 3). The steric energy for the conformation was calculated to be 488 kcal/mol. Compared to the steric energy of the optimized conformation (−1.42 kcal/mol, Supporting Information Figure S7), an input energy of at least 488 kcal/mol is needed. According to the calculation by Efremenko and Sheintuch, the adsorption energy for phenol on graphite plane is −3.1 kcal/mol (*30*). BPA has two phenol groups and would have adsorption energy of ∼ −6.2 kcal/mol, which is much lower than the energy required to compensate the energy for conformational change. Hence, the flat configuration is unlikely the main mode of adsorption. However, the benzene rings around the circumference of CNTs have a certain angle depending on the tube diameter. BPA could be adsorbed with two benzene rings on the benzene rings in fullerene (BPA 4 in Figure 3) and CNTs (BPA 2 in Figure 3) along circumferential or diagonal direction. However, as presented in Supporting Information Figure S8, for the CNTs with larger diameter, a wider angle between two benzene rings of BPA is required, and a higher steric energy has to be spent for the change of BPA molecular conformation. This conformational change is less favorable, then, BPA would have only one benzene ring adsorbed on CNMs, which makes it more like EE2, which further explains that the adsorption difference between EE2 and BPA decreased as the diameter of CNMs increased.

Adsorption Mechanism. The much higher K values of EE2 could be attributed to higher hydrophobicity of EE2 than BPA. Normalization of K values by hexadecane-water partition coefficient (K_{HW}) could screen out hydrophobic effect, and thus other potential adsorption mechanism could be discussed (*31*). The resulted parameter, K/K_{HW}, is listed in Supporting Information Table SII. The normalized adsorption coefficient (K/K_{HW}) of EE2 showed only about 1.5 times higher than BPA on CNTs, but BPA had a higher K/K_{HW} on fullerene than EE2. The adsorption of EE2 was observed to decrease with increased pH, but no pH dependence was observed for BPA (Supporting Information Figure S9). These data show that hydrogen bonding could not be excluded in EE2 adsorption, and should not be a predominant mechanism for BPA adsorption on CNMs (*32*). This is possible because CNM surface may contain some oxygen-containing functional groups during purification using HNO_3/H_2SO_4. However, contribution of hydrogen bonding to the overall adsorption of EE2 is unknown.

The $\pi-\pi$ bond has been shown to be a dominating interaction force for the adsorption of chemicals containing benzene rings on CNMs (*32, 33*). Compared to our previous study on polyaromatic hydrocarbon (PAHs) adsorption on MWCNT15 (*15*), the K/K_{HW} values of EE2 and BPA are 6 orders of magnitude higher than PAHs (Supporting Information Figure S10). K/K_{HW} for PAHs follow the order of naphthalene < phenanthrene < pyrene, which is consistent with the order of benzene ring numbers. This observation implies that $\pi-\pi$ bond is an important force for PAH adsorption on CNMs. However, difference in benzene ring numbers could not explain the higher adsorption of EE2 and BPA. The $\pi-\pi$ complex has been shown to be very strong for electron donor–acceptor systems, but weak for pairs of donors or acceptors (*32, 34*). The phenol group is a charge donor, and CNMs could be either donor or acceptor (*28*). Therefore, the $\pi-\pi$ bond formed between EE2 or BPA and CNMs is a donor–acceptor system, and much stronger than that between PAHs and CNMs.

Adsorption/Desorption Hysteresis. Adsorption/desorption hysteresis was generally observed for both chemicals on CNMs (Figures 4, S12, and S13). The sorption coefficients increased 2 to 20 times for the third desorption cycle compared to those for adsorption. Nonequilibrated adsorption is a typical artifact for desorption hysteresis, and the increased adsorption could be simply attributed to prolonged contact time. In our both adsorption and desorption systems, equilibrium reached within 5 days according to our preliminary work. Therefore, nonequilibrium is not the cause for the hysteresis in this study. Loss of sorbate, such as degradation, evaporation, and particle loss during desorption, is another reason for artifact hysteresis. A direct quantification of adsorbate on solid phase was conducted in order to rule out this artifact. The solid particles were extracted three times by methanol, and the calculated recovery for our adsorption/desorption system was from 88 to 110%. This reasonably high recovery confirmed the validity of mass balance calculation. In addition, no degradation of either of the

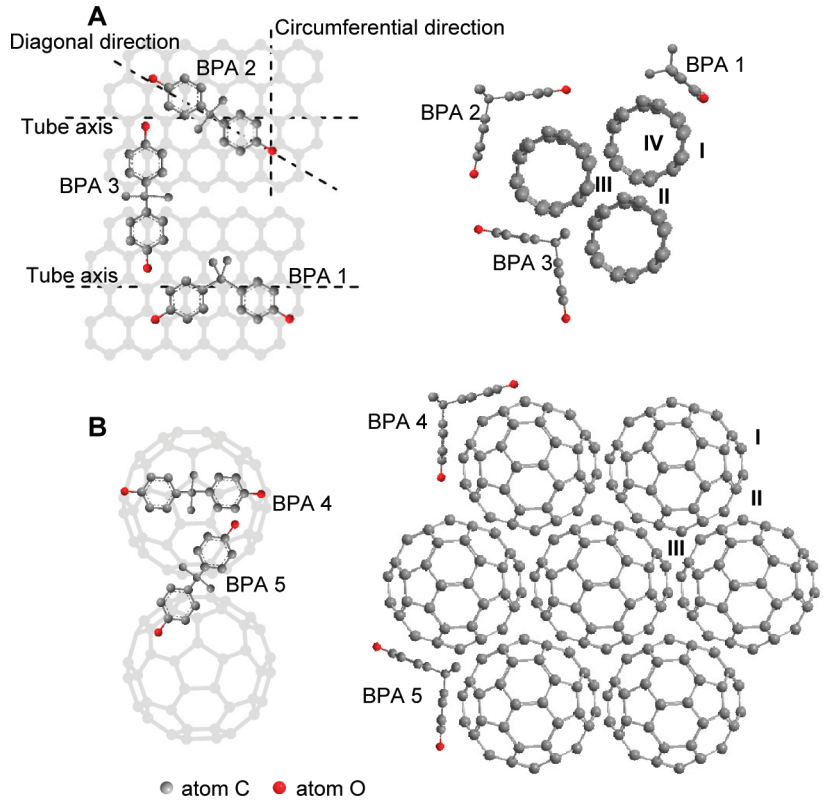

FIGURE 3. Schematic diagrams for adsorption of BPA on SWCNT (A) and fullerene (B). The letters I, II, III, and IV indicate the possible adsorption areas of surface, groove, interstitial spaces, and inner pores, respectively. One type of armchair CNTs, SWCNT (3, 3) is presented as an example. The adsorption of EDCs on other types of CNTs (such as zigzag CNT) could be easily followed. BPA 1 is adsorbed on CNT with two benzene rings in the direction of tube axis. BPA 2 and BPA 4 show the adsorption on the surface, whereas BPA 3 and BPA 5 illustrate the wedging of this molecule in the groove area. The interstitial space is too small for the molecules to fit.

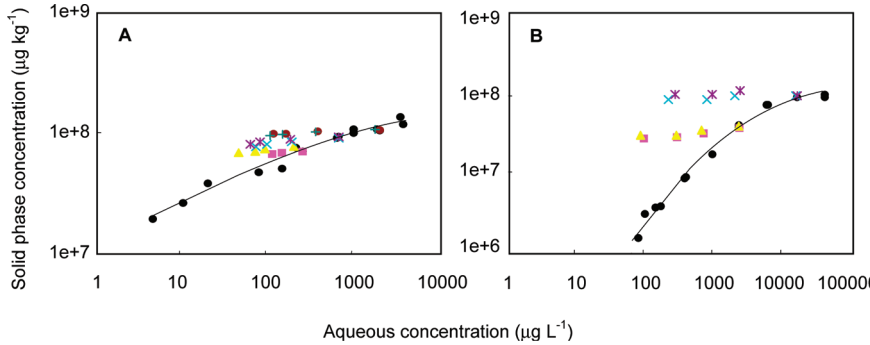

FIGURE 4. Adsorption isotherms of EE2 (A) and BPA (B) on MWCNT15. Solid lines are the fitting curves using PMM. Color points are desorption curves. Desorption hysteresis is significant for all the points, and the similar desorption hysteresis could be found in Supporting Information Figures S12 and S13 for the other CNMs.

chemicals was observed as indicated by clean HPLC chromatograms during adsorption/desorption processes. Therefore, the adsorption/desorption hysteresis observed in this study is the true hysteresis. Hysteresis has been observed in adsorption/desorption systems, such as naphthalene−fullerene (*35*), cyclopentane vapor−fullerene (*36*), and PAHs−fullerene (*37*), and in pressure induced infiltration/defiltration system for paraxylene sorption on MWCNT (*38*). However, the hysteresis was not significant for PAHs on CNTs (*37*).

Desorption hysteresis was widely reported for organic contaminants from soils/sediments, and was attributed to irreversible pore deformation of the adsorbent by the adsorbate and the formation of meta-stable states of adsorbate in fixed mesopores (*39, 40*). The porous structure is swelled during adsorption and collapsed during desorption. Therefore, desorption takes place in a different pathway from adsorption. A similar explanation was employed to explain the adsorption/desorption hysteresis on CNMs. As suggested by Yang and Xing, rearrangement of fullerene aggregates resulted in the formation of new closed interstitial spaces (*37*). Rathousky and Zukal speculated that the sorbate penetrated into the bulk of fullerene crystals and localized in the octahedral interstices between fullerene molecules (*36*). Thus, both rearrangement of aggregates and penetration of sorbate into closed interstitial spaces are responsible for desorption hysteresis. Zhao et al. reported that the molecules with small charge transfer and weak binding did not cause any change of SWCNT electronic properties after adsorption, but for molecules with considerable charge transfer and strong adsorption, both electronic band structures and density of state significantly changed after adsorption (*28*). They also showed the redistribution of electron density of a single SWCNT after the interaction with NO_2 molecules, and they concluded that the interaction between individual

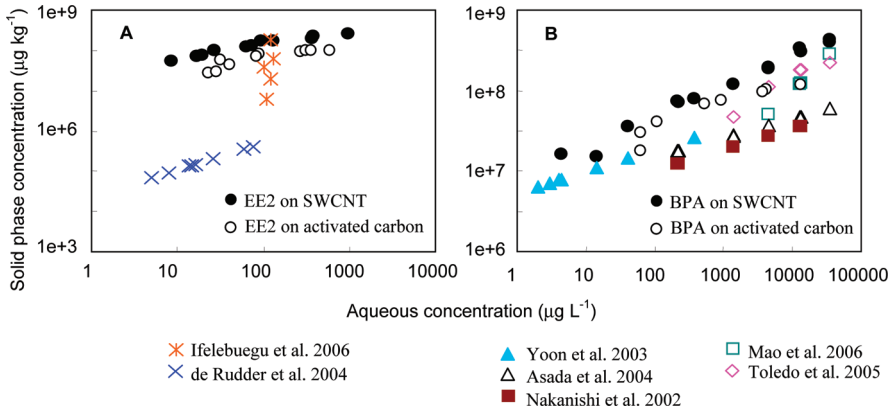

FIGURE 5. Comparison of EE2 (A) and BPA (B) adsorption on activated carbons and SWCNT. Both solid and open circles are the experimental data in this study, whereas the other points are calculated from literature results. Several different types of activated carbon were involved in the cited papers. Only the one with the highest adsorption was selected to compare with SWCNT. The data points are calculated from the parameters in their experimental concentration ranges.

SWCNTs could also be changed after NO_2 adsorption. Similarly, the bundles or aggregates of CNMs could be rearranged after adsorption of EE2 and BPA in this study, resulting in a different path way between adsorption and desorption. However, this type of change is expected to be much less for molecules with weaker adsorption (such as PAHs < BPA). Therefore, desorption hysteresis is observed for EE2 and BPA which have much stronger adsorption (Supporting Information Figure S10).

Potential Application of CNMs in Water Treatment. Conventional physical removal, such as coagulation, flocculation, and sedimentation, has been reported to be ineffective in removing pharmaceuticals including EDCs (*41*). Therefore, many studies have been conducted to optimize adsorption-based water treatment procedures. Activated carbon-based method has been proven to be very effective to remove many EDCs from water (*42, 43*). Criteria of adsorbent applicability for water treatment is generally based on adsorption capacity and kinetics (*44*). Adsorption by SWCNT and activated carbon was compared in Figure 5. SWCNT showed slightly higher adsorption of both BPA and EE2 than the activated carbon used this study, but much higher than activated carbons from literature results.

Superior adsorption characteristics of SWCNT over activated carbons for water treatment were also reported in literature. For example, Lu et al. reported a higher adsorption and shorter equilibrium time needed for trihalomethanes on carbon nanotubes than activated carbon (*45*). Using a technique based on temperature-programmed desorption, Long and Yang observed desorption energy of dioxin adsorbed by carbon nanotubes 3 times higher than that by activated carbon and 7 times higher than that by γ-Al_2O_3 (*46*). They speculated high dioxin removal efficiency by carbon nanotubes. Su and Lu studied the adsorption kinetics and thermodynamics of natural dissolved organic matter (NDOM) on CNTs (*17*). Their results showed a higher adsorption capacity of NDOM and less weight loss after 10 cycles of water treatment and reactivation for SWCNT than activated carbon. In addition, because of the strong oxidation resistance and rigid structure, SWCNT could be used for a longer time than activated carbons. All these studies along with our results indicate that SWCNT could be a potential adsorbent for water treatment. However, extended studies are needed on the operational side such as SWCNT bed-packing, separation from aqueous phase, and recycling.

Supporting Information Available

EE2 and BPA properties (Table SI); Fitting results of the isotherms for EE2 and BPA adsorption on CNMs (Table SII); Distribution of relative errors for solid phase concentration as fitted using Freundlich model (Figure S1); Fitting results of EE2 and BPA adsorption on CNMs using FM (Figures S2 and S3); Fitting results of EE2 and BPA adsorption on CNMs using LM (Figures S4 and S5); Correlation of adsorption coefficient (K) with specific surface area (SSA) (Figure S6); Optimized 3-dimensional structures of EE2 and BPA based on minimized steric energy (Figure S7); The steric energy for different conformations of BPA with two benzene rings forming different angles (Figure S8); Adsorption of EE2 and BPA on CNMs as affected by pH (Figure S9); Comparison of K/K_{HW} between PAHs and EDCs (Figure S10); Relationships between K_{HW} and K_{OW} for both polyaromatic hydrocarbons (PAHs) and alkylated phenols (APs) (Figure S11); Desorption hystereis of EE2 adsorbed on CNMs (Figure S12); Desorption hystereis of BPA adsorbed on CNMs (Figure S13). This material is available free of charge via the Internet at http://pubs.acs.org.

Acknowledgments

This research was supported by the Massachusetts Water Resource Center (2007MA73B) and Massachusetts Agricultural Experiment Station (MA 90).

Literature Cited

(1) Snyder, S. A.; Westerhoff, P.; Yoon, Y.; Sedlak, D. L. Pharmaceuticals, personal care products, and endocrine disruptors in water: Implications for the water industry. *Environ. Eng. Sci.* **2003**, *20*, 449–469.

(2) Daughton, C. G.; Ternes, T. A. Pharmaceuticals and personal care products in the environment: Agents of subtle change. *Environ. Health Perspect.* **1999**, *107*, 907–938.

(3) de Rudder, J.; Van de Wiele, T.; Dhooge, W.; Comhaire, F.; Verstraete, W. Advanced water treatment with manganese oxide for the removal of 17 alpha-ethynylestradiol (EE2). *Water Res.* **2004**, *38*, 184–192.

(4) Andersen, H. R.; Hansen, M.; Kjolholt, J.; Stuer-Lauridsen, F.; Ternes, T.; Halling-Sorensen, B. Assessment of the importance of sorption for steroid estrogens removal during activated sludge treatment. *Chemosphere* **2005**, *61*, 139–146.

(5) Holbrook, R. D.; Love, N. G.; Novak, J. T. Sorption of 17-beta-estradiol and 17 alpha-ethinylestradiol by colloidal organic carbon derived from biological wastewater treatment systems. *Environ. Sci. Technol.* **2004**, *38*, 3322–3329.

(6) Tsai, W. T.; Lai, C. W.; Su, T. Y. Adsorption of bisphenol-A from aqueous solution onto minerals and carbon adsorbents. *J. Hazard. Mater.* **2006**, *134*, 169–175.

(7) Toledo, I. B.; Ferro-Garcia, M. A.; Rivera-Utrilla, J.; Moreno-Castilla, C.; Fernandez, F. J. V. Bisphenol A removal from water by activated carbon. Effects of carbon characteristics and solution chemistry. *Environ. Sci. Technol.* **2005**, *39*, 6246–6250.

(8) Asada, T.; Oikawa, K.; Kawata, K.; Ishihara, S.; Iyobe, T.; Yamada, A. Study of removal effect of bisphenol A and beta-estradiol by porous carbon. *J. Health Sci.* **2004**, *50*, 588–593.

(9) Nakanishi, A.; Tamai, M.; Kawasaki, N.; Nakamura, T.; Tanada, S. Adsorption characteristics of bisphenol A onto carbonaceous materials produced from wood chips as organic waste. *J. Colloid Interface Sci.* **2002**, *252*, 393–396.
(10) Ifelebuegu, A. O.; Lester, J. N.; Churchley, J.; Cartmell, E. Removal of an endocrine disrupting chemical (17 alpha-ethinyloestradiol) from wastewater effluent by activated carbon adsorption: Effects of activated carbon type and competitive adsorption. *Environ. Technol.* **2006**, *27*, 1343–1349.
(11) Yoon, Y. M.; Westerhoff, P.; Snyder, S. A.; Esparza, M. HPLC-fluorescence detection and adsorption of bisphenol A, 17 beta-estradiol, and 17 alpha-ethynyl estradiol on powdered activated carbon. *Water Res.* **2003**, *37*, 3530–3537.
(12) Mao, M.; Liu, Z. B.; Wang, T.; Yu, B. Y.; Wen, X.; Yang, K. G.; Zhao, C. S. Polysulfone-activated carbon hybrid particles for the removal of BPA. *Sep. Sci. Technol.* **2006**, *41*, 515–529.
(13) Stackelberg, P. E.; Gibs, J.; Furlong, E. T.; Meyer, M. T.; Zaugg, S. D.; Lippincott, R. L. Efficiency of conventional drinking-water-treatment processes in removal of pharmaceuticals and other organic compounds. *Sci. Total Environ.* **2007**, *377*, 255–272.
(14) Hu, J. Y.; Chen, X.; Tao, G.; Kekred, K. Fate of endocrine disrupting compounds in membrane bioreactor systems. *Environ. Sci. Technol.* **2007**, *41*, 4097–4102.
(15) Yang, K.; Zhu, L. Z.; Xing, B. S. Adsorption of polycyclic aromatic hydrocarbons by carbon nanomaterials. *Environ. Sci. Technol.* **2006**, *40*, 1855–1861.
(16) Pyrzynska, K.; Stafiej, A.; Biesaga, M. Sorption behavior of acidic herbicides on carbon nanotubes. *Microchim. Acta* **2007**, *159*, 293–298.
(17) Su, F. S.; Lu, C. S. Adsorption kinetics, thermodynamics and desorption of natural dissolved organic matter by multiwalled carbon nanotubes. *J. Environ. Sci. Health Part A:Toxic/Hazard. Subst. Environ. Eng.* **2007**, *42*, 1543–1552.
(18) Li, Y. H.; Wang, S. G.; Wei, J. Q.; Zhang, X. F.; Xu, C. L.; Luan, Z. K.; Wu, D. H.; Wei, B. Q. Lead adsorption on carbon nanotubes. *Chem. Phys. Lett.* **2002**, *357*, 263–266.
(19) Li, Y. H.; Wang, S. G.; Zhang, X. F.; Wei, J. Q.; Xu, C. L.; Luan, Z. K.; Wu, D. H. Adsorption of fluoride from water by aligned carbon nanotubes. *Mater. Res. Bull.* **2003**, *38*, 469–476.
(20) Cai, Y. Q.; Jiang, G. B.; Liu, J. F.; Zhou, Q. X. Multi-walled carbon nanotubes packed cartridge for the solid-phase extraction of several phthalate esters from water samples and their determination by high performance liquid chromatography. *Anal. Chim. Acta* **2003**, *494*, 149–156.
(21) Segner, H.; Navas, J. M.; Schafers, C.; Wenzel, A. Potencies of estrogenic compounds in in vitro screening assays and in life cycle tests with zebrafish in vivo. *Ecotox. Environ. Safe.* **2003**, *54*, 315–322.
(22) Braga, O.; Smythe, G. A.; Schafer, A. I.; Feitz, A. J. Fate of steroid estrogens in Australian inland and coastal wastewater treatment plants. *Environ. Sci. Technol.* **2005**, *39*, 3351–3358.
(23) Staples, C. A.; Dorn, P. B.; Klecka, G. M.; O'Block, S. T.; Harris, L. R. A review of the environmental fate, effects, and exposures of bisphenol A. *Chemosphere* **1998**, *36*, 2149–2173.
(24) Oehlmann, J.; Schulte-Oehimann, U.; Bachmann, J.; Oetken, M.; Lutz, I.; Kloas, W.; Ternes, T. A. Bisphenol A induces superfeminization in the ramshorn snail *Marisa cornuarietis* (Gastropoda: Prosobranchia) at environmentally relevant concentrations. *Environ. Health Perspect.* **2006**, *114*, 127–133.
(25) Pan, B.; Xing, B. S.; Liu, W. X.; Tao, S.; Lin, X. M.; Zhang, X. M.; Zhang, Y. X.; Xiao, Y.; Dai, H. C.; Yuan, H. S. Distribution of sorbed phenanthrene and pyrene in different humic fractions of soils and importance of humin. *Environ. Pollut.* **2006**, *143*, 24–33.
(26) Pan, B.; Xing, B. S.; Liu, W. X.; Tao, S.; Lin, X. M.; Zhang, Y. X.; Yuan, H. S.; Dai, H. C.; Zhang, X. M.; Xiao, Y. Two-compartment sorption of phenanthrene on eight soils with various organic carbon contents. *J. Environ. Sci. Health Part B: Pestic. Contam. Agric. Wastes* **2006**, *41*, 1333–1347.
(27) Trubiano, G.; Borio, D.; Ferreira, M. L. Ethyl oleate synthesis using Candida rugosa lipase in a solvent-free system. Role of hydrophobic interactions. *Biomacromolecules* **2004**, *5*, 1832–1840.
(28) Zhao, J. J.; Buldum, A.; Han, J.; Lu, J. P. Gas molecule adsorption in carbon nanotubes and nanotube bundles. *Nanotechnology* **2002**, *13*, 195–200.
(29) Pearce, J. V.; Adams, M. A.; Vilches, O. E.; Johnson, M. R.; Glyde, H. R. One-dimensional and two-dimensional quantum systems on carbon nanotube bundles. *Phys. Rev. Lett.* **2005**, 95.
(30) Efremenko, I.; Sheintuch, M. Predicting solute adsorption on activated carbon: Phenol. *Langmuir* **2006**, *22*, 3614–3621.
(31) Borisover, M.; Graber, E. R. Classifying NOM - Organic sorbate interactions using compound transfer from an inert solvent to the hydrated sorbent. *Environ. Sci. Technol.* **2003**, *37*, 5657–5664.
(32) Chen, W.; Duan, L.; Zhu, D. Q. Adsorption of polar and nonpolar organic chemicals to carbon nanotubes. *Environ. Sci. Technol.* **2007**, *41*, 8295–8300.
(33) Gotovac, S.; Hattori, Y.; Noguchi, D.; Miyamoto, J.; Kanamaru, M.; Utsumi, S.; Kanoh, H.; Kaneko, K. Phenanthrene adsorption from solution on single wall carbon nanotubes. *J. Phys. Chem. B* **2006**, *110*, 16219–16224.
(34) Zhu, D. Q.; Hyun, S. H.; Pignatello, J. J.; Lee, L. S. Evidence for pi-pi electron donor-acceptor interactions between pi-donor aromatic compounds and pi-acceptor sites in soil organic matter through pH effects on sorption. *Environ. Sci. Technol.* **2004**, *38*, 4361–4368.
(35) Cheng, X. K.; Kan, A. T.; Tomson, M. B. Naphthalene adsorption and desorption from Aqueous C-60 fullerene. *J. Chem. Eng. Data* **2004**, *49*, 675–683.
(36) Rathousky, J.; Zukal, A. Adsorption of krypton and cyclopentane on C-60: An experimental study. *Fullerene Sci. Technol.* **2000**, *8*, 337–350.
(37) Yang, K.; Xing, B. S. Desorption of polycyclic aromatic hydrocarbons from carbon nanomaterials in water. *Environ. Pollut.* **2007**, *145*, 529–537.
(38) Punyamurtula, V. K.; Qiao, Y. Hysteresis of sorption isotherm of multiwall carbon nanotube in paraxylene. *Mater. Res. Innovations* **2007**, *11*, 37–39.
(39) Sander, M.; Lu, Y. F.; Pignatello, J. J. A thermodynamically based method to quantify true sorption hysteresis. *J. Environ. Qual.* **2005**, *34*, 1063–1072.
(40) Braida, W. J.; Pignatello, J. J.; Lu, Y. F.; Ravikovitch, P. I.; Neimark, A. V.; Xing, B. S. Sorption hysteresis of benzene in charcoal particles. *Environ. Sci. Technol.* **2003**, *37*, 409–417.
(41) Ternes, T. A.; Meisenheimer, M.; McDowell, D.; Sacher, F.; Brauch, H. J.; Gulde, B. H.; Preuss, G.; Wilme, U.; Seibert, N. Z. Removal of pharmaceuticals during drinking water treatment. *Environ. Sci. Technol.* **2002**, *36*, 3855–3863.
(42) Snyder, S. A.; Adham, S.; Redding, A. M.; Cannon, F. S.; DeCarolis, J.; Oppenheimer, J.; Wert, E. C.; Yoon, Y. Role of membranes and activated carbon in the removal of endocrine disruptors and pharmaceuticals. *Desalination* **2007**, *202*, 156–181.
(43) Kim, S. D.; Cho, J.; Kim, I. S.; Vanderford, B. J.; Snyder, S. A. Occurrence and removal of pharmaceuticals and endocrine disruptors in South Korean surface, drinking, and waste waters. *Water Res.* **2007**, *41*, 1013–1021.
(44) Mestre, A. S.; Pires, J.; Nogueira, J. M. F.; Carvalho, A. P. Activated carbons for the adsorption of ibuprofen. *Carbon* **2007**, *45*, 1979–1988.
(45) Lu, C. S.; Chung, Y. L.; Chang, K. F. Adsorption of trihalomethanes from water with carbon nanotubes. *Water Res.* **2005**, *39*, 1183–1189.
(46) Long, R. Q.; Yang, R. T. Carbon nanotubes as superior sorbent for dioxin removal. *J. Am. Chem. Soc.* **2001**, *123*, 2058–2059.

ES8001184